SOME RESULTS OF GROUND-BASED HIGH-RESOLUTION SPECTROSCOPY OF THE MARTIAN ATMOSPHERE. Vladimir A. Krasnopolsky, Catholic University of America (Department of Physics, 200 Hannan Hall, Washington, DC 20064, vkrasn@verizon.net).

Introduction: High-resolution spectroscopy of the martian atmospheres is a powerful tool to study the chemical composition and its variations by mapping of species using long-slit spectrographs. Ground-based observations have significantly contributed to the study of the chemical composition of Mars' atmosphere (Table 1).

Table 1. Chemical composition of the Martian atmosphere. Spacecraft data are in black, ground-based spectroscopy is in red, spectroscopy from Earth-orbiting observatories in blue.

Species	Mixing ratio	Instrument
CO_2	0.955	GS
N_2	0.027	Viking/MS
Ar	0.016	Viking/MS
Ne	2.5 ppm	Viking/MS
Kr	0.3 ppm	Viking/MS
Xe	80 ppb	Viking/MS
H	2.7×10^{4} cm^{-3}	Mariner/UVS
O	0.01-0.02	Mariner/UVS
O_2	$(1.2–2)\times10^{-3}$	FPI
CO	8×10^{-4}	FTS
H_2O	0–70 pr. μm	GS
O_3	0–60 μm-atm	Mariner/UVS
He	10 ppm	EUVE
H_2	17 ppm	FUSE
HDO/H_2O	1.7×10^{-3}	CFHT/FTS
HD	12 ppb	HST/GHRS
H_2O_2	0–40 ppb	IRTF/TEXES
CH_4	10 ppb	CFHT/FTS
H_2S	< 100 ppb	Mariner/IRIS
HCl	< 2 ppb	KPNO/FTS
H_2CO	< 3 ppb	KPNO/FTS
SO_2	< 1 ppb	IRTF/TEXES
NO	< 1.7 ppb	IRTF/TEXES

GS is grating spectrometer, MS mass spectrometer, FPI Fabry-Perot interferometer, FTS Fourier transform spectrometer.

Mapping of the O_2 Dayglow at 1.27 μm. This dayglow is a sensitive tracer of Mars' photochemistry and can be observed with the NASA IRTF/CSHELL long-slit spectrograph. The proposed observations were made by Krasnopolsky and Bjoraker [1], Novak et al. [2], and Krasnopolsky [3, 4]. A seasonal-latitudinal map of the dayglow intensity for the entire martian year from [4] is shown in Fig. 1.

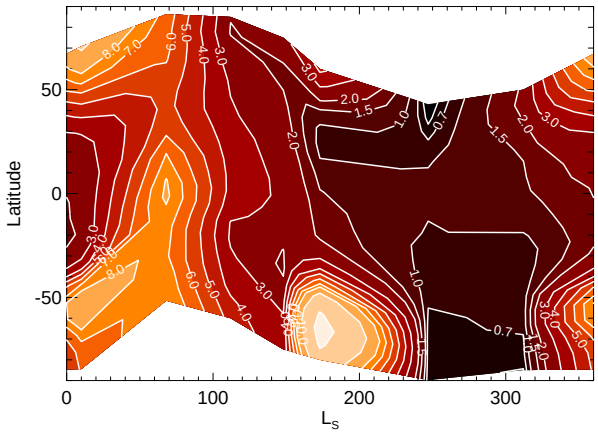

Fig. 1. Seasonal- latitudinal map of the O_2 dayglow at 1.27 μm (in MR). From Krasnopolsky [4].

The O_2 dayglow at 1.27 μm is currently observed using the SPICAM-IR spectrometer (Korablev et al. [5]) at the Mars Express orbiter. Results of the observations for the first martian year (Fedorova et al. [6]) corrected for variations with local time are in reasonable agreement with the data in Fig. 1.

Photochemical Modeling of Variations of O_3, H_2O_2, and the O_2 Dayglow. Photochemical general circulation models may be the best tool for modeling of variations of photochemical products on Mars. The published models of this type (Lefevre et al. [7], Moudden and McConnell [8]) do not involve the O_2 dayglow at 1.27 μm and aim mostly at variations of ozone.

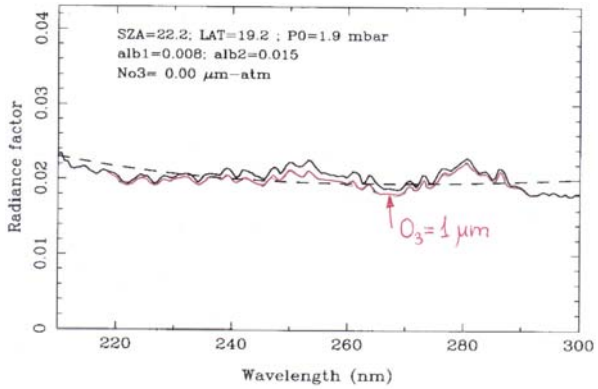

Fig. 2. SPICAM UV spectrum above Olympus Mons (solid line) and its smoothed version (dashed line) used as a reference spectrum for extraction of ozone from the observations. From Perrier et al. [9]. Red line shows the same spectrum with O_3 = 1 μm-atm.

There is a significant difference between the SPICAM UV nadir observations of ozone (Perrier et al. [9]) and the O_3 abundances from the ground-based infrared heterodyne (Fast et al. [10, 11]) and HST UV (Clancy et al. [12]) observations at low and middle latitudes. Extraction of O_3 abundances from the UV spectra requires some assumptions on the spectral behavior of the surface reflectivity and dust scattering that may significantly affect the results (Fig. 2).

Krasnopolsky [13] made a 1D model for variations of photochemical products at low and middle latitudes on Mars using the long-term MGS/TES observations of temperature profiles, H_2O, and dust and ice aerosol (Smith [14, 15]). The model involves a weak heterogeneous loss of H_2O_2 on the water ice aerosol. The model results are in very good agreement with the ground-based observations (Fig. 3).

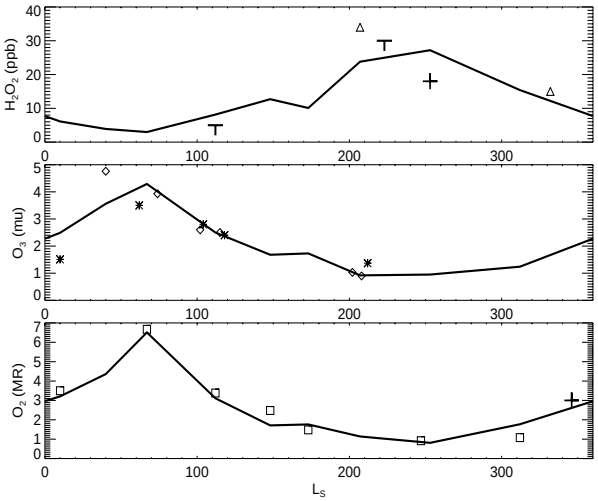

Fig. 3. Seasonal variations of the O_2 dayglow intensity and O_3 and H_2O_2 abundances at low and middle latitudes. Solid lines: model [13], squares are from [4], diamonds [10], asterisks [12], triangles [16, 17]. Plus in the lower panel is from [18] and in the upper panel from [19]. Two upper limits are from [20, 21]. From Krasnopolsky [13].

Methane on Mars. Methane on Mars was detected using CFHT/FTS (Krasnopolsky et al. [22, 23]) and then PFS at Mars Express (Formisano et al [24]). The first of these publications [22] with the basic information on the retrieved abundance, lifetime, and possible sources was submitted before the beginning of the science observations at Mars Express. The detected abundance 10 ± 3 ppb is, however, very near the standard detection criterion 3 sigma. Recent attempt to detect methane and its variations using IRTF/CSHELL resulted in an upper limit of 14 ppb (Fig. 4, Krasnopolsky [4]).

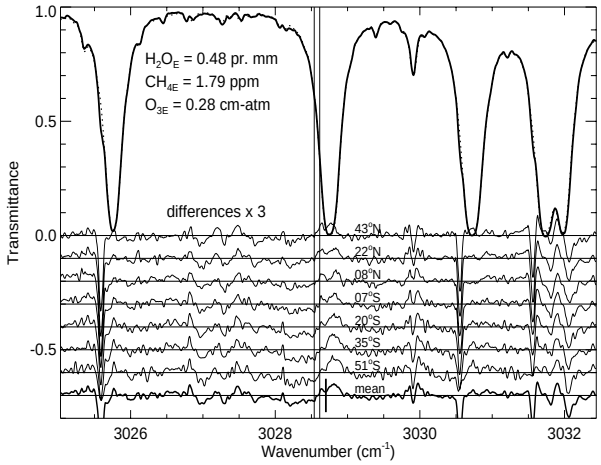

Fig. 4. Spectrum of Mars near the R0 line of CH_4 and differences between the observed and synthetic spectra for seven latitudes. The expected position of the martian R0 line is shown by two vertical lines. No methane has been observed with an upper limit of 14 ppb. Abundances of telluric H_2O, CH_4, and O_3 are derived from the spectrum. From Krasnopolsky [4].

There are two controversial issues regarding methane on Mars: its variations and origin. Briefly, methane may vary on Mars if its heterogeneous loss is more effective than that on the Earth by a factor of >1000 [25]. However, the expected loss is higher on the Earth because of the liquid ocean and the abundant O_2. Therefore, some claimed variations of CH_4 on Mars may be observational artifacts. The observed abundances of peroxide are rather low, its total production by the dust devils is low as well [13], and there are no laboratory data on the oxidation of CH_4 by H_2O_2. Therefore, this mechanism is highly questionable.

Considering geological sources of methane on Mars, the following facts should be taken into account [25]: (1) lack of current volcanism, (2) lack of warm spots (Mars Odyssey/THEMIS), and (3) low seepage of gases from the interior from the lack of $SO_2 < 1$ ppb. These facts strengthen the biological source of methane.

Seasonal, Latitudinal, and Solar Cycle Variations of CO. Latitudinal variations of CO were detected for the first time by Krasnopolsky [26] at L_S = 112º using IRTF/CSHELL at 1.57 μm. The revealed new effect was properly explained as due to condensation and sublimation of CO_2 on the polar regions. This effect should involve all long-living incondensable species (N_2, Ar, O_2, CO, and H_2). One and half year later this effect and its interpretation was confirmed by the observations of Ar using GRS at Mars Odyssey orbiter (Sprague et al. [27, 28]). The observations of

CO were continued in [4] and resulted in a map in Fig. 5. Recently Mars Express observed seasonal variations of CO over Hellas [26] that are generally consistent with the data in Fig. 5. All these results are relevant to dynamics of the polar processes and circulation on Mars and may be used to test GCMs.

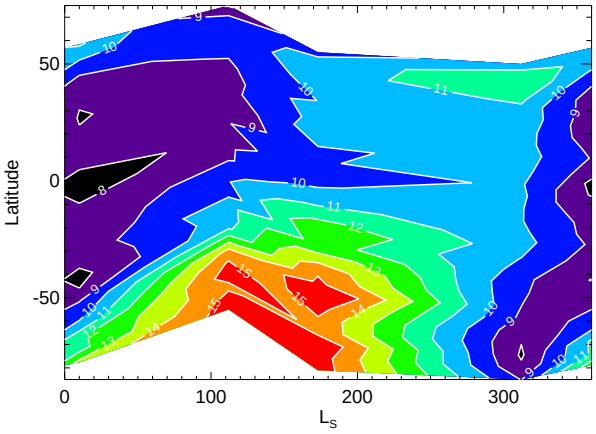

Fig. 5. Seasonal-latitudinal variations of the CO mixing ratio (in 10^{-4}). From Krasnopolsky [4].

Long-term variations of the total CO abundance on Mars (Fig.6) is another result of the observations. These variations are driven by the 11-year solar cycle and in reasonable agreement with the model prediction [30]: a time delay is 1.24 years, amd a maximum to minimum ratio is 1.21.

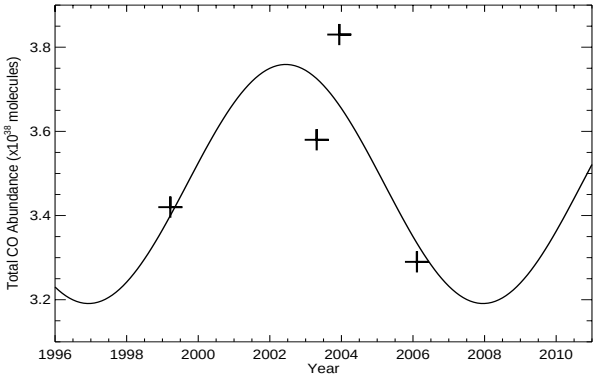

Fig. 6. Variations of the total CO abundance with the 11-year solar cycle.

Carbon and Oxygen Isotope Ratios in CO_2. The required accuracy of the isotope ratios is very high (~1%) and difficult to achieve because of uncertainties associated with (1) equivalent widths of the observed lines, (2) line strengths in spectroscopic databases, and (3) thermal structure of the martian atmosphere above the observed regions.

To solve the problem, Krasnopolsky et al. [31] observed a spectrum of Mars at 1.6 μm with resolving power of 5×10^5 using the CFHT/FTS. This spectrum (Fig. 7) includes ~200 lines of each CO_2 isotope. (A final uncertainty is in inverse proportion to square root of the line number.) High-precision laboratory studies of line strengths of the isotopic CO_2 lines near 1.6 μm have been made as well. Finally, data of MGS/TES and two GCM models [32, 33] on the thermal structure of the martian atmosphere and its variations have been applied to reduce uncertainties of the isotope ratios. The obtained isotope ratios are

$$^{13}C/^{12}C = 0.978 \pm 0.020$$
$$^{18}O/^{16}O = 1.018 \pm 0.018$$

times the terrestrial standards. The retrieved ratios show that isotope fractionation between CO_2 and oxygen and carbon reservoirs in the solid phase is almost balanced by nonthermal escape and sputtering of O and C on Mars. These ratios may be used to study evolution of volatiles on Mars with a better confidence.

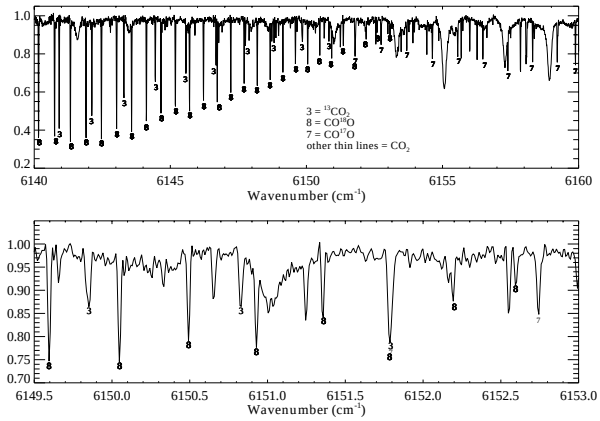

Fig. 7. Small parts (7% and 1.2%) of the CFHT/FTS spectrum with numerous lines of the CO_2 isotopes. From Krasnopolsky et al. [31].

Acknowledgment. This work is supported by the NASA Planetary Astronomy Program.

References: [1] Krasnopolsky V.A. and Bjoraker G.L. (2000) *JGR 105*, 20179. [2] Novak R.E. et al. (2002) *Icarus 158*, 14. [3] Krasnopolsky V.A. (2003) *Icarus 165*, 315. [4] Krasnopolsky V.A. (2007) *Icarus 190*, 93. [5] Korablev O. et al. (2006) *JGR 111*, E09S03. [6] Fedorova A. et al. (2007) *JGR 111*, E09S07. [7] Lefevre F. et al. (2004) *JGR 109*, E07004. [8] Moudden Y. and McConnell J.C. (2007) *Icarus 188*, 18. [9] Perrier S. et al. (2006) *JGR 111*, E09S06. [10] Fast K. et al. (2006) *Icarus 181*, 419. [11] Fast K. et al. (2006) *Icarus 183*, 396. [12] Clancy R.T. et al. (1999) *Icarus 138*, 49. [13] Krasnopolsky V.A. (2006) *Icarus 185*, 153. [14] Smith M.D. (2002) *JGR 107*, 5115. [15] Smith M.D. (2004) *Icarus 167*, 148. [16] Encrenaz T. et al. (2004) *Icarus 170*, 424. [17] Encrenaz T. et al. (2008) *Icarus 195*, 547. [18] Traub W.A. et al. (1979) *ApJ 229*, 846. [19] Clancy R.T. et

al. (2004) *Icarus 168*, 116. [20] Krasnopolsky V.A. et al. (1997) *JGR 102*, 6525. [21] Encrenaz T. et al. (2002) *A&A 396*, 1037. [22] Krasnopolsky V.A. et al. (2004) EGU04-A-06169. [23] Krasnopolsky V.A. et al. (2004) *Icarus 172*, 537. [24] Formisano V. et al. (2004) *Science 306*, 1758. [25] Krasnopolsky V.A. (2006) *Icarus 180*, 359. [26] Krasnopolsky V.A. (2003) *JGR 108*, E2, 5010. [27] Sprague A.L. et al. (2004) *Science 306*, 1364. [28] Sprague A.L. et al. (2007) *JGR 112*, E03S02. [29] Encrenaz T. et al. (2006) *A&A 459*, 265. [30] Krasnopolsky (1993) *Icarus 101*, 33. [31] Krasnopolsky V.A. et al. (2007) *Icarus 190*, 93. [32] Forget F. et al. (1999) *JGR 104*, 24155. [33] Hartogh P. et al. (2005) *JGR 110*, E11008.